Theoretical Calculation of the Interaction of Hydrogen with Models of Coordinatively Unsaturated Centers on Alumina

Dan Fărcaşiu* and Povilas Lukinskas

Department of Chemical and Petroleum Engineering, University of Pittsburgh, 1249 Benedum Hall, Pittsburgh, Pennsylvania 15261

Received: March 17, 1999; In Final Form: June 30, 1999

Ab initio calculations with large basis sets and electron correlation were conducted on the reaction of hydrogen molecules with $(HO)_3Al(OH_2)_x$ clusters, where $x = 0$, 1, and 2. In this way, the reactivity of Al(III) species was studied as a function of their level of coordinative unsaturation. For the tricoordinated species, the geometry of the starting cluster was obtained by the optimization of the species $(HO)_3Al(OH_2)_{x+1}$ and removal of the extra water molecule, on the basis of idea that aluminum oxide surfaces are formed by calcination of hydrated forms. Two models, one assuming rigidity and the other allowing for flexibility of the tricoordinated aluminum center, were examined. The complexes with physisorbed and chemisorbed hydrogen were optimized in the same way. The reactions of tetra- and pentacoordinated aluminum clusters were studied without any constraints on the geometry. The calculations predicted the hydrogen chemisorption to be endothermic in all cases, the order being $E(x = 0) < E(x = 1) < E(x = 2)$. The chemisorption pathway was investigated and its transition structure and energy barrier were established. The energy barriers for chemisorption, determined as the relative energies of the transition structures E_{TS}, varied with the coordination number of the aluminum atom as $E_{TS}(x = 0) < E_{TS}(x = 1) < E_{TS}(x = 2)$. The barriers were similar for the rigid and for the flexible tricoordinated aluminum clusters. A significant conclusion is that tetracoordinated sites on alumina must be thought of as reactive (if not *the* reactive) sites. The literature description (on the basis of ab initio calculations with small basis sets at the HF level) of hydrogen chemisorption as an acid−base reaction, involving hydrogen heterolysis concerted with the attachment of the proton to oxygen (basic site) and the hydride to aluminum (acid site), is not substantiated by our calculations. Instead, the chemisorption occurs through the interaction of H_2 with the aluminum (metal ion catalysis) until both hydrogen atoms are bonded to Al, after which one of the hydrogens migrates to an adjacent oxygen atom. B3LYP calculations give results in reasonable agreement with the MP2 calculations, attesting to the appropriateness of the density functional theory method for these types of structures.

Introduction

The ability of transitional aluminas to exchange the hydrogens in their composition with gas-phase D_2 molecules at high temperatures is well-established.[1] The reaction mechanism was not actually established, but it was discussed [2] in connection with the hydrogen "spillover" from a noble metal catalyst to the support.[3] It is agreed that the reaction involves the coordinatively unsaturated aluminum atoms, which are also the Lewis acid centers,[1e,4] but the nature of the reaction is different from the standard Lewis acid−Lewis base interaction. We note that the noble metal atoms, which are highly active in dissociating hydrogen molecules and bonding the hydrogen atoms, do not react as Lewis acids. Chloridated aluminas give the same level of hydrogen adsorption as the untreated oxides.[2d,5] The activation energies measured were low for both γ- and η-alumina, but indications of diffusion control were obtained.[1c−e]

Other workers have attempted to model the hydrogen chemisorption on alumina by molecular-orbital calculations, both semiempirical [6] and ab initio.[4b,7] The alumina was modeled by minimal-size clusters (one aluminum atom). For the model of the tricoordinated reactive site, $Al(OH)_3$ (**1**), the reaction can be described by eq 1, in which a complex with physisorbed hydrogen (**2**) is the intermediate in the generation of the complex with chemisorbed hydrogen (**3**).[4b] The ab initio calculations[8] were conducted with small basis sets at the Hartree−Fock level.[4b,7]

$$\underset{\mathbf{1}}{H_2 + Al(OH)_3} \rightleftarrows \underset{\mathbf{2}}{H_2\cdots Al(OH)_3} \rightleftarrows \underset{\mathbf{3}}{H-Al(OH)_2(-OH_2)} \quad (1)$$

The main reasults of the previous calculations were (a) a strong hydrogen physisorption (−7 kcal/mol), (b) a highly exothermic (−26.5 kcal/mol) hydrogen chemisorption, and an energy barrier of only 2.5 kcal/mol relative to the reactants (**1** + H_2).[7] As the most important point, however, the reaction was described as an acid−base mechanism, involving heterolysis of the H−H bond, synchronous with the bonding of the proton to the oxygen (basic site) and the hydride to aluminum (acid site).[7]

In our work on carbocations, we had noticed that neglect of electron correlation leads in some cases to the misidentification of energy minima and transition states.[9] Because we found the acid−base mechanism of hydrogen dissociation intriguing, we decided to reinvestigate the reaction of hydrogen with aluminum hydroxide clusters, using larger basis sets and electron correlation. Another important goal was to investigate the reactivity of Al(III) species in hydrogen chemisorption as a function of the coordination number of aluminum. We chose to study models of the sites on alumina, rather than the alumina itself,

* To whom correspondence should be addressed. Tel.: 412-624-7449. Fax 412-624-9639. E-mail: dfarca@vms.cis.pitt.edu.

10.1021/jp990939a CCC: $18.00
Published on Web 10/01/1999

because (a) we were dealing with an irregular surface and (b) we were not seeking to model most accurately the energies of chemisorption, but to establish its mechanism. Indeed, the application of periodic boundary conditions presumes that the entire unit cell including the reactants is periodically repeated,[10] whereas the sites which we wanted to model are defect sites. Also, there are no reliable experimental adsorption or activation energies with which to compare the results, as mentioned above. Embedding the structural moiety into the surface should have more of an effect on the energies of reaction and activation than on the mechanism of reaction and relative reactivity of sites of different structure. We can also cite the observation that the errors from neglect of long-range electrostatic effects are less important than the errors from inadequate optimization of structures.[11] We felt that it was most important to use large basis sets.

Finally, another problem was examined. We had found earlier that the results of density functional theory (DFT) calculations do not always match those obtained with standard ab initio calculations.[12] It was, therefore, important to check whether the former is satisfactory in a problem of the kind studied here, which would make more complex systems, for instance with larger reactants than hydrogen, amenable to study with appropriately large basis sets.

Computational Method

The calculations were conducted with the program Gaussian 94,[13] in the manner described previously.[14] All geometry optimizations were conducted with electron correlation with the MP2 method or with the DFT-B3LYP[15] method. The 6-31G*, 6−31-G**, 6-31++G**, 6-311G**, and 6-311++G** basis sets were used. For optimization of controlled geometries, symmetry constraints were used in some cases and "dummy" atoms were used in others.[11] The energies reported below were not corrected for zero point energies. Tests in a few cases indicated that those corrections (1−4 kcal/mol) are too small to affect the conclusions. No correction for the basis set superposition errors (BSSE) was attempted.[16] Some literature data indicate that the BSSE might not be important for large basis sets, particularly when diffuse functions are included.[17] In our calculations, the energies of the physisorbed complexes would be affected by this omission.

The optimization of the transition structures for the adsorption to the tricoordinated aluminum complex **1** with fixed bond angles and dihedral angles (mode A, see below) were conducted with the Synchronous Transit-Guided Quasi-Newton (STQN) method.[18] For the alternative description of the cluster, in which the hydrogen atoms in $Al(OH)_3$ (**1**) were fixed throughout the reaction of eq 1 (mode B), the transition structures were optimized with the standard Berny optimization; a geometry close to that found for the analogous transition structure (A) was used as the first guess. The transition structure for the reaction of **1** in mode B with plane of symmetry imposed could not be optimized by either method. Each transition state was checked by frequency analyses.[8c] Intrinsic reaction coordinate (IRC)[19] tracking was conducted at the MP2/6-31G** level (step size: 2.0 $amu^{-1/2}$ bohr, maximum number of steps: 15). For the reaction of **1** in mode A with no symmetry restrictions, IRC tracking was also conducted at the MP2/6-31++G** level, because the transition structure obtained without the inclusion of diffuse functions was different from those obtained in all other cases.

The Berny optimization was also used for the transition structures of the chemisorption on clusters with tetracoordinated and pentacoordinated aluminum atoms. The first guess was based on the assumption that the transition structure would be similar to that found for the cluster with tricoordinated aluminum (**1**). The results were checked by frequency analyses and IRC tracking.

The projections of the molecular geometry shown here were generated with the computer programs XMOL[20] and MOLDEN. Assignment of calculated frequencies to specific vibration modes was performed with the computer program MOLDEN.[21]

Results and Discussion

1. Cluster Model Selection. The first matter which had to be addressed in our study was the choice of the aluminum hydroxide cluster. The coordinatively unsaturated centers on alumina surfaces are considered to contain tricoordinated and pentacordinated aluminum atoms.[4b,22] Tricoordinated aluminum centers were considered to exist in significant concentration and even dicoordinated $-O-Al^{+}-O-$ centers were said to be present.[23] An NMR study with cross-polarization from chemisorbed ammonia molecules evidenced, however, only tetra-, penta-, and hexacoordinated aluminum atoms in aluminas and in the intracavity material of steamed zeolites.[24] The authors concluded that the theoretical considerations "in which trigonal Al is the working horse are not experimentally founded."[21] A theoretical evaluation of the electric field gradient in alumina also considered only tetra-, penta-, and hexacoordinated aluminum atoms, of which only the pentacoordinated atoms were deemed to represent the Lewis acid sites.[25] In this context, the previous calculations of hydrogen chemisorption become questionable, because in one of them only the tricoordinated species $Al(OH)_3$ was considered,[7] whereas in the other work, the pentacoordinated cluster $Al(OH)_5$ was also examined but did not bind hydrogen.[4b] It was not clear from the latter paper whether the species considered was the dianion $Al(OH)_5^{2-}$ or a dioxidized, electrically neutral species of the same formula, but neither of them appears to us to be a good choice. We decided to compare the reactivity toward hydrogen of sites with tri-, tetra- and pentacoordinated aluminum atoms and for that purpose we considered in our calculations clusters of the formula $(HO)_3Al(OH_2)_x$, where $x = 0$, 1, and 2, thus avoiding both negatively charged and unnatural, oxidized models.

The tetracoordinated aluminum sites are not normally considered as Lewis acid sites. The ^{15}N NMR spectrum of pyridine-^{15}N adsorbed on γ-alumina has identified, however, two types of Lewis acid sites.[26] Because it was shown that the concentration of tricoordinated aluminum in that material is nil or vanishingly small,[21] it is at least plausible that some tetracoordinated sites possess Lewis acidity.

The second important point was to choose a geometry of the clusters which would best model the sites on the alumina surface. The previous calculations had employed a cluster in which the bond angles and dihedral angles in the $Al(O)_3$ fragment of the $Al(OH)_3$ were frozen in the regular tetrahedral geometry and only the Al−O bond lengths were optimized. The Al−O−H angles were in one study frozen at the same value as the Al−O−Al angles.[4b] No indication on this matter was given in the other study, but from the drawings shown it appears that the O−H bonds were frozen in a similar orientation.[7] The Al−O bond lengths, optimized in both cases at the HF/3-21G level, were 1.681[7] and 1.730 Å,[4b] but not enough information was provided in either case to comment on this otherwise disturbing discrepancy. The chemisorption was predicted to be highly exothermic, −26.6[7] and −30.4 kcal/mol.[4b,27] The regular tetrahedron geometry is unrealistic, however, for a tricoordinated

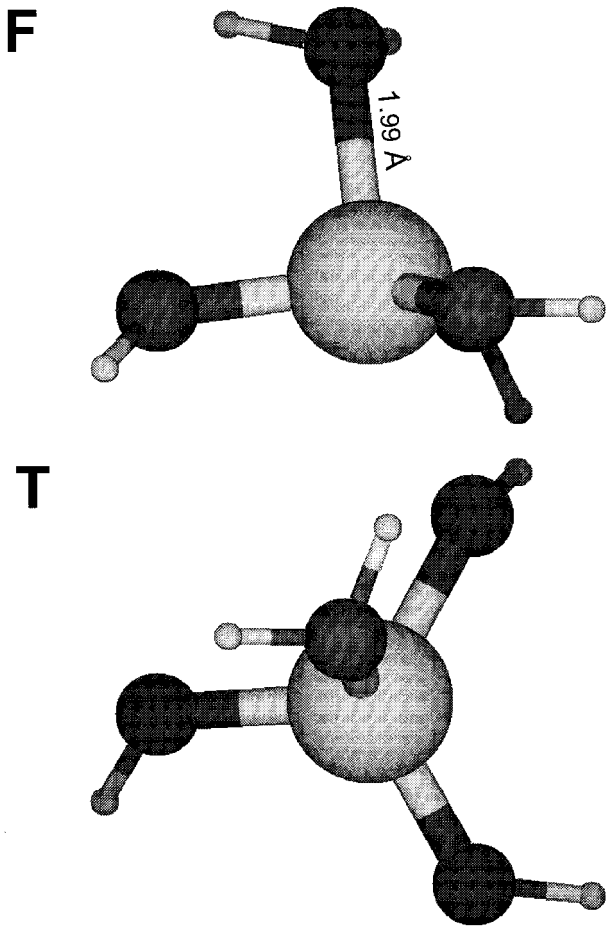

Figure 1. The geometry of the complex of $Al(OH)_3$ with water, **1** (**4**, $x = 0$), calculated at the B3LYP/6-311++G** level. F: front view; T: top view.

aluminum atom. Our full optimization of **1** at the MP2/6-31G** level gave a planar structure (dihedral angle φ(O1−Al−O2−O3) = 180°), with the hydrogens oriented in a helix (3-fold symmetry, C_{3h}). The calculations indicated that **1** does not bind (chemisorb) hydrogen, if the planar geometry is maintained. If the adduct **3** is fully optimized (MP2/6-31G**), it acquires a distorted tetrahedral geometry (φ(O1−Al−O2−O3) = 87.3°). For the fully optimized geometries of both **1** and **3**, the process of eq 1 is endothermic by 3.6 kcal/mol. Finally, if the $Al(OH)_3$ geometry is frozen as in the optimum geometry of **3**, the reaction is exothermic by 45 kcal/mol.

For the choice of an appropriate model geometry, we started from the consideration that transitional aluminas are formed by the calcination of a hydrated aluminum oxide, like boehmite. We can write the hydrated form of the primitive clusters as $(HO)_3Al(OH_2)_{x+1}$ (**4**) and their dehydration by eq 2. For $x = 0$, we optimized the geometry of the hydrated cluster **4** ($x = 0$) as the starting point and then removed the extra water molecule to obtain the corresponding reactive (coordinatively unsaturated) cluster.

$$\underset{\mathbf{4}}{(HO)_3(H_2O)_xAl\text{–}OH_2} \longrightarrow (HO)_3(H_2O)_xAl + H_2O \qquad (2)$$

Geometry optimization of **4**, $x = 0$, indicated that the disposition of the $(HO)_3Al$ fragment before dehydration (Figure 1) is flatter than in the regular tetrahedral arrangement, the dihedral angle φ(O1−Al−O2−O3) being ca. 155° at all levels of theory. Any geometry change upon the elimination of water would result in an even flatter geometry, because the most stable geometry of $(HO)_3Al$ (**1**) is planar, as noted above.

An appropriate model of the tricoordinated aluminum center on the surface is then intermediate between the tetrahedral and planar structures of **1**. One can consider that the bulk of the solid is already set to a significant extent at the boehmite stage and the structural reorganization upon calcination affects mostly the surface. Therefore, the geometry of the reactive cluster with $x = 0$ (**1**) was optimized with constraints, in two modes. In the first (A), the bond angles and dihedral angles around the aluminum atom were frozen as in **4**, $x = 0$, and the other geometrical parameters of the dehydrated cluster were optimized. In the alternative mode (B), the rigidity of the solid was simulated by freezing the hydrogen atoms in the positions which they had in the hydrated cluster **4**, $x = 0$, then optimizing the geometry of the central part of the cluster (the $Al(-O-_*)_3$ group) after the removal of the extra water. This allowed a "breathing" movement of the $Al(-O-)_3$ group.

The examination of the reaction of clusters **1** (tricoordinated), $(HO)_3Al(OH_2)$ (**5**, tetracoordinated), and $(HO)_3Al(OH_2)_2$ (**6**, pentacoordinated) with hydrogen (eq 3) involved the calculation of structures and energies of the reactants (**1**, **5**, and **6**) and products (**3**, **7**, and **8**), as well as of the intermediates with physisorbed hydrogen (**2**, **9**, and **10**) and of the transition structures for the chemisorption step (**11**−**13**). For $x = 0$, all the species were examined in both modes A and B. Because the tetra- and pentacoordinated clusters have a lower conformational mobility than the tricoordinated clusters, the optimizations of the corresponding species ($x = 1$, $x = 2$) were performed without constraints. We can note that a model of the pentacoordinated site with the geometry frozen as a truncated octahedron (i.e., a square pyramid with the aluminum in the center of the base) did not chemisorb hydrogen in earlier published calculations.[4b]

$$\underset{\mathbf{1}\ \mathbf{5}\ \mathbf{6}}{H\text{–}H + (HO)_3Al(OH_2)_x} \longrightarrow \underset{\mathbf{2}\ \mathbf{9}\ \mathbf{10}}{H\text{–}H\cdots(HO)_3Al(OH_2)_x} \longrightarrow \underset{\mathbf{11}\ \mathbf{12}\ \mathbf{13}}{\left[H\cdots H\cdots(HO)_3Al(OH_2)_x\right]^{\ddagger}} \longrightarrow \underset{\mathbf{3}\ (x=0)\ \ \mathbf{7}\ (x=1)\ \ \mathbf{8}\ (x=2)}{HO\text{–}Al(\text{–}H)(OH_2)_x(HO)(H_2O)} \qquad (3)$$

2. Reaction of Tricoordinated Aluminum Clusters. An extensive series of calculations were conducted on the reaction of eq 3, $x = 0$, with the constraints described in mode A, above. It was observed that rotations around the Al−OH bonds occur upon optimization, such as to bring each hydrogen atom close to an oxygen other than the one to which it is bonded. Because it is not clear whether such a movement would be possible in the solid during the dehydration step, we also conducted a series of calculations in which two of the Al−O−H groups were disposed symmetrically relative to the plane determined by Al and the third O−H bond. The calculations were run with several basis sets, from MP2/6-31G* to MP2/6-311++G**,[8c] to determine the effect of the basis set size. A parallel series of calculations with the same basis sets were run with the B3LYP method, to determine whether the DFT is satisfactory for this type of calculation. The results are presented in Table 1.

TABLE 1: Relative Energies of Species Involved in the Addition of Hydrogen to the Tricoordinated Aluminum Cluster (2), in kcal/mol[a]

level of theory		6-31G*	6-31G**	6-31++G**	6-311G**	6-311++G**
			mode A, no symmetry constraint			
physisorbed complex	MP2	−1.13	−1.53	−1.20	−2.78	−1.97
	B3LYP	−1.23	−1.78	−1.08	−2.18	−1.44
transition structure	MP2	(22.80)[b]	(19.31)[b]	26.87	(17.26)[b]	24.55
	B3LYP	(18.58)[b]	(16.69)[b]	23.54	(16.71)[b]	23.36
chemisorbed complex	MP2	20.34	17.93	20.52	15.80	18.37
	B3LYP	17.26	15.65	18.61	15.69	17.78
			mode A, plane of symmetry			
physisorbed complex	MP2	−1.92	−3.13	−3.13	−4.23	−3.87
	B3LYP	−2.47	−3.26	−2.76	−3.59	−3.15
transition structure	MP2	27.41	22.49	24.11	19.61	21.84
	B3LYP	22.03	18.93	20.67	18.13	20.26
chemisorbed complex	MP2	16.52	14.21	16.40	11.56	14.34
	B3LYP	13.95	12.45	14.50	11.35	13.72
			mode B, no symmetry constraint			
physisorbed complex	MP2		(−1.05)[c]			
	B3LYP		−	−0.19		
transition structure	MP2		27.38	−		
	B3LYP		−	23.13		
chemisorbed complex	MP2			−		
	B3LYP		5.28	2.93		
			mode B, plane of symmetry			
physisorbed complex	MP2		−1.84			
	B3LYP		−			
transition structure	MP2		−			
	B3LYP		−			
chemisorbed complex	MP2		4.63			
	B3LYP		3.75			

[a] The sum of the energies of reactants, **2** and H_2, is taken as zero. [b] This does not represent the actual transition structure for the hydrogen chemisorption; see text. [c] The energy surface was very flat; the energy change per pass was in the range of 10^{-6} Hartrees when the optimization was stopped.

The results show that the interactions involved in the hydrogen physisorption (**1** → **2**) are very weak and are of the van der Waals type. The value of nearly −7 kcal/mol obtained in the earlier report[7,27] might be the result of the geometry constraints imposed upon the system. The shortest Al ··· H distance for the complex optimized in mode A was 2.2−2.7 Å. On the other hand, the chemisorbed complex **3** is a high-energy species, even though it is a bona fide energy minimum. This finding represents a dramatic reversal of the prediction of the previous calculations.[4b,7] Nevertheless, the energy barrier which we calculate for hydrogen exchange is similar to the value reported by the previous authors (actually smaller than it),[7] but the rate-determining step predicted there was the *desorption* of hydrogen, rather than adsorption, as we find here. The calculated energies change with the increase in the basis set, but the changes are not dramatic and do not affect the conclusions. The same qualitative picture of the reaction results from the calculations at the MP2/6-31G* level and at the MP2/6-311G** level. Therefore, the former can give acceptable results in cases where the size of the system prevents the use of larger basis sets. The introduction of diffuse functions raises the energy for both the physisorbed and chemisorbed complexes. The large differences between the energy barriers calculated with and without diffuse functions in the basis set result from the fact that the latter do not identify correctly the transition structure, as will be discussed below.

Calculations in mode A with the imposition of a plane of symmetry lowered the energy of **3**, but not that of **11**. The barrier calculated for hydrogen exchange remains, therefore, the same.

Calculations in mode B as defined above allowed a significant degree of flexibility to the Al(−O−)$_3$ group. The dihedral angle φ(O1−Al−O2−O3) in **1** was 170−175°, close to the planar value, whereas in **3** it was 96−114°, close to tetrahedral. The interaction with hydrogen was difficult to follow, because the energy surface of the physisorbed complex was extremely flat and convergence failure frequently occurred. Optimization of structures for all steps (structures **2**, **11**, and **3**) was achieved for the system without a plane of symmetry, at the MP2/6-31G** level and B3LYP/6-31++G** level (Table 1). It appears that there is a relationship between the closeness to planarity of the center and the strength of physisorption. Thus, the complex without symmetry constraint shown in Figure 2, is the closest to planarity, φ(O1−Al−O2−O3) = 177.2°, and has the weakest interaction with the molecular hydrogen, 0.19 kcal/mol, at the equilibrium distance of 3.01 Å (longest of all cases involving **1**). On the other hand, because of the increased flexibility of the reactive cluster in this mode (B), the stability of the chemisorbed complex, shown in Figure 3, is very much increased, although its formation is still endothermic. The energy of the transition structure, that is, the barrier for hydrogen dissociation and exchange does not change, however, from mode A to mode B. Calculations of the cluster in mode B with the imposition of a plane of symmetry were conducted for the structures **2** and **3** at the MP2/6-31G** level and for **3** at the B3LYP/6-31G** level, with results similar to those obtained without the imposition of a plane of symmetry (Table 1).

The bond lengths in the chemisorbed complexes were similar in all cases: Al−H ca. 1.61 Å, O−H ca. 0.96 Å, and the Al−O bond involved in the chemisorption stretched from 1.73 to ca. 2.0 Å.

3. Reaction of the Tetracoordinated and Pentacoordinated Aluminum Clusters. The van der Waals complex (**9**) of cluster **5** with hydrogen was a local minimum and the equilibrium distance was 3.40−3.61 Å, in all cases. The energy of physisorption (1−2 kcal/mol, Table 2) was similar to the values for the tricoordinated aluminum cluster (**1**). The chemisorption

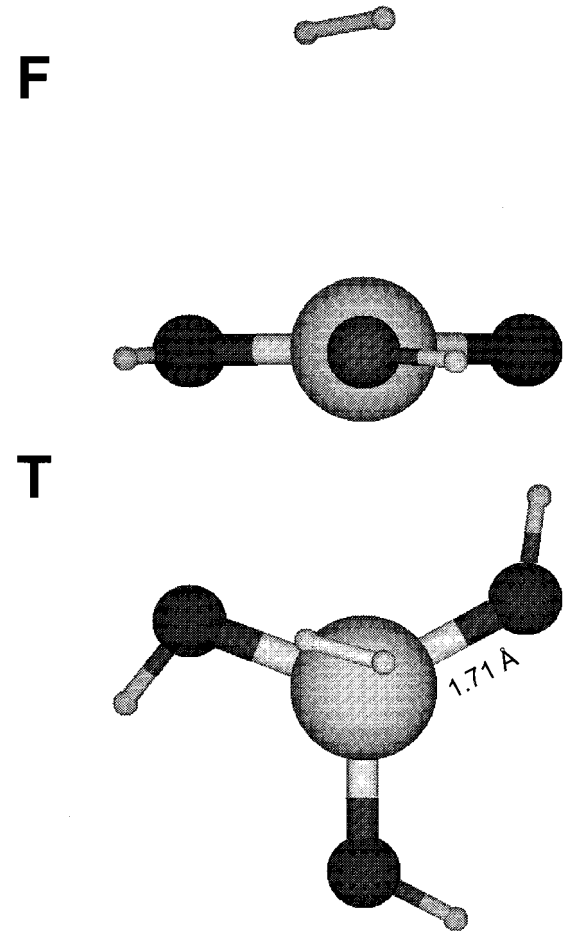

Figure 2. The complex with hydrogen physisorbed on the tricoordinated aluminum cluster (**2**), optimized in mode B with no symmetry constraint, at the B3LYP/6-31++G** level. F, T as in Figure 1.

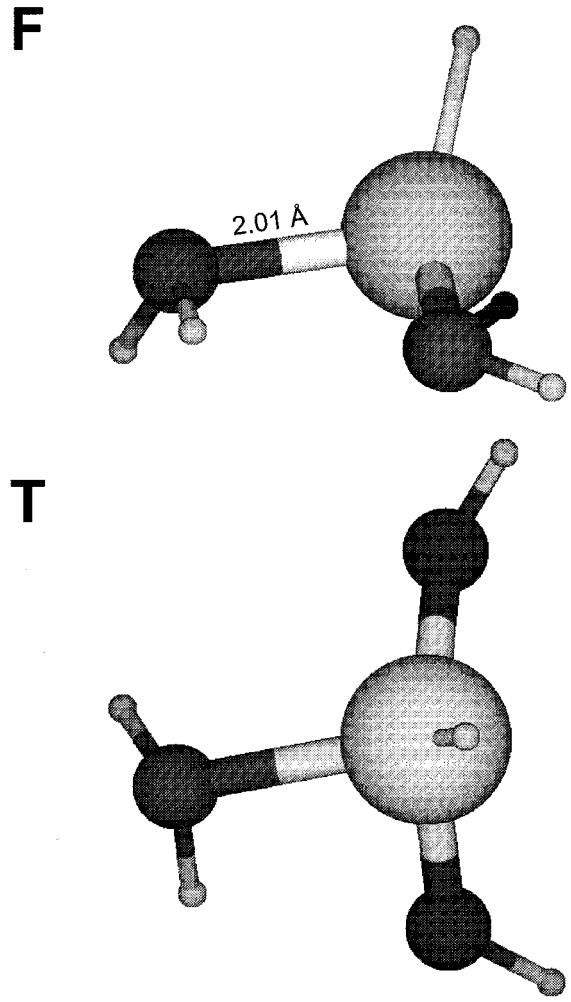

Figure 3. The complex with hydrogen chemisorbed on the tricoordinated aluminum cluster (**3**) optimized in mode B with no symmetry constraint, at the B3LYP/6-31++G** level. F, T as in Figure 1.

of hydrogen on cluster **5** (eq 3, $x = 1$) can give six stereoisomeric adducts **7**. On the basis of the results obtained for the larger cluster **6** (below) only the stereoisomer with the two water ligands in apical positions (trans from each other, **7a**) was studied (Table 2). The adduct with one water ligand and the hydrogen ligand in apical positions (**7b**) was briefly examined at the B3LYP/6-31++G** level, but after eight optimization cycles it had expelled the apical water ligand (d_{Al-O} increased to 2.54 Å), thus going to **3**. As shown in Table 2, the relative energy of the chemisorbed complex (**7a**) is lower than that for the tricoordinated cluster in mode A, but higher than that for the more flexible cluster, mode B. The relative energy of the transition structure **12** is higher than that of the smaller-size analogue **11**. The geometry of the adduct **7a** is shown in Figure 4.

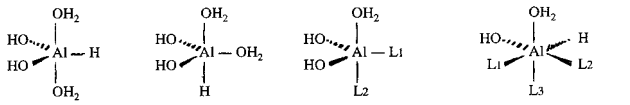

To study the reaction of the pentacoordinated aluminum cluster, we examined two of the three possible stereoisomers of the reactant: with the two water ligands apical, apical (**6a**) and apical, equatorial (**6b**) in the trigonal bipyramid. The isomer **6a** was more stable at the MP2/6-31G** and B3LYP/6-31G** levels, by about 3 kcal/mol. The isomer **6b**, with adjacent water molecules, optimized to a very distorted structure, intermediate between **6b** and **6c** (water ligands equatorial, equatorial). At the B3LYP/6-31++G** level, only **6a** was an energy minimum; the other isomer decomposed to **5** and one molecule of water. The relative energies given in Table 2 are calculated relative to **6a** and a hydrogen molecule.

TABLE 2: Relative Energies of Species Involved in the Addition of Hydrogen to Tetra- (3) and Pentacoordinated Aluminum Clusters (4), in kcal/mol[a]

level of theory		6−31G**	6−31++G**
tetracoordinated cluster $Al(OH)_3(OH_2)$			
physisorbed complex (**9**)	MP2	−1.71	
	B3LYP	−2.04	−1.07
transition structure (**12**)	MP2	33.59	
	B3LYP	30.11	32.78
chemisorbed complex (**7a**)	MP2	14.25	
	B3LYP	13.47	14.75
pentacoordinated cluster $Al(OH)_3(OH_2)_2$			
physisorbed complex (**10**)	MP2	(−0.65)[b]	
	B3LYP	−0.79	−0.03
transition structure (**13**)	MP2	44.20	
	B3LYP	40.96	38.94
chemisorbed complex (**8a**)	MP2	29.65	
	B3LYP	28.31	27.15

[a] The sum of the energies of reactants, **2** and H_2, is taken as zero. [b] The optimization was stopped when the value of the maximum forces on the nuclei in the internal coordinates was smaller than 10^{-3}.

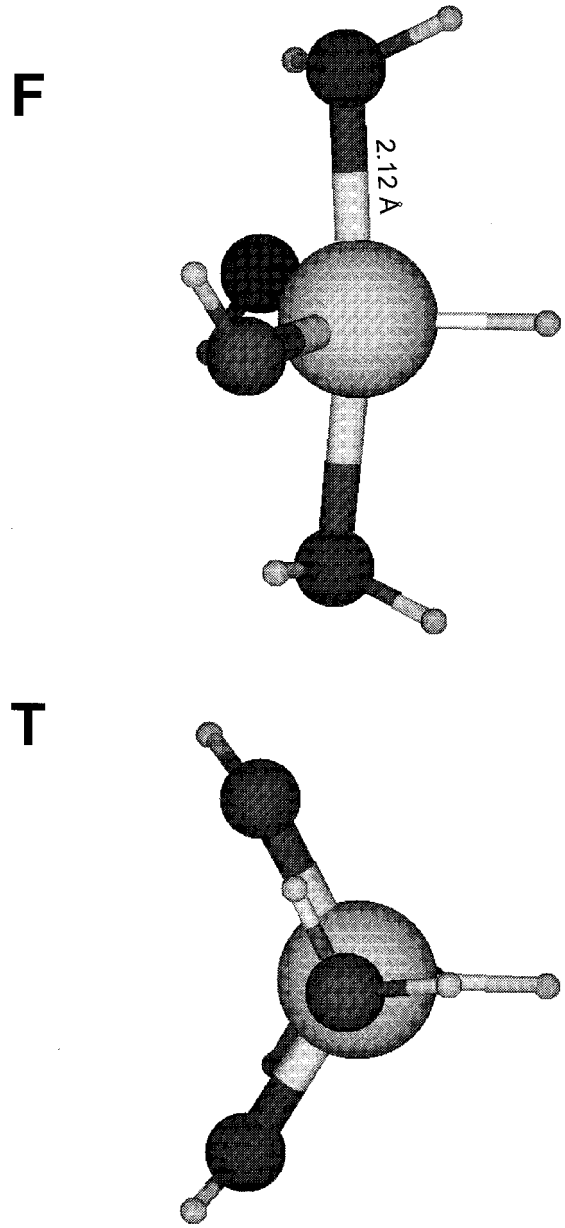

Figure 4. B3LYP/6-31++G** geometry of the complex of the tetracoordinated aluminum cluster with chemisorbed hydrogen (**7a**). F, T as in Figure 1.

Hydrogen physisorption to **6a** gave a weak complex (0−0.8 kal/mol interaction energy), with a long equilibrium distance (4.1−5.2 Å at various levels of theory). Of the three possible chemisorbed complexes, **8a**, **8b**, and **8c**, of the pentacoordinated reactive cluster, only **8a** and **8b**, which had two water ligands trans from each other, were stable at the MP2/6-31G** level, but **8b** decomposed by expelling water at B3LYP/6-31G** and B3LYP/6-31++G** levels. This behavior reflects, most likely, the mutual repulsion of like charges, because **8a** had the OH groups trans from one another. Even the isomer **8a** was a weak complex, as shown by the high relative energy (Table 2) and one long Al−OH_2 bond (ca 2.3 Å). Only the transition structure for the formation of **8a** was, therefore, optimized (**13a**). It can be seen in Table 2 that both the energy of the chemisorbed complex and the barrier for its formation are much higher for the pentacoordinated aluminum cluster than for the tetracoordinated cluster.

4. The Transition Structure for Hydrogen Chemisorption. The search for the transition structure in the chemisorption at cluster **1** in mode A with no symmetry constraints and the basis sets without diffuse functions located a saddle point structurally

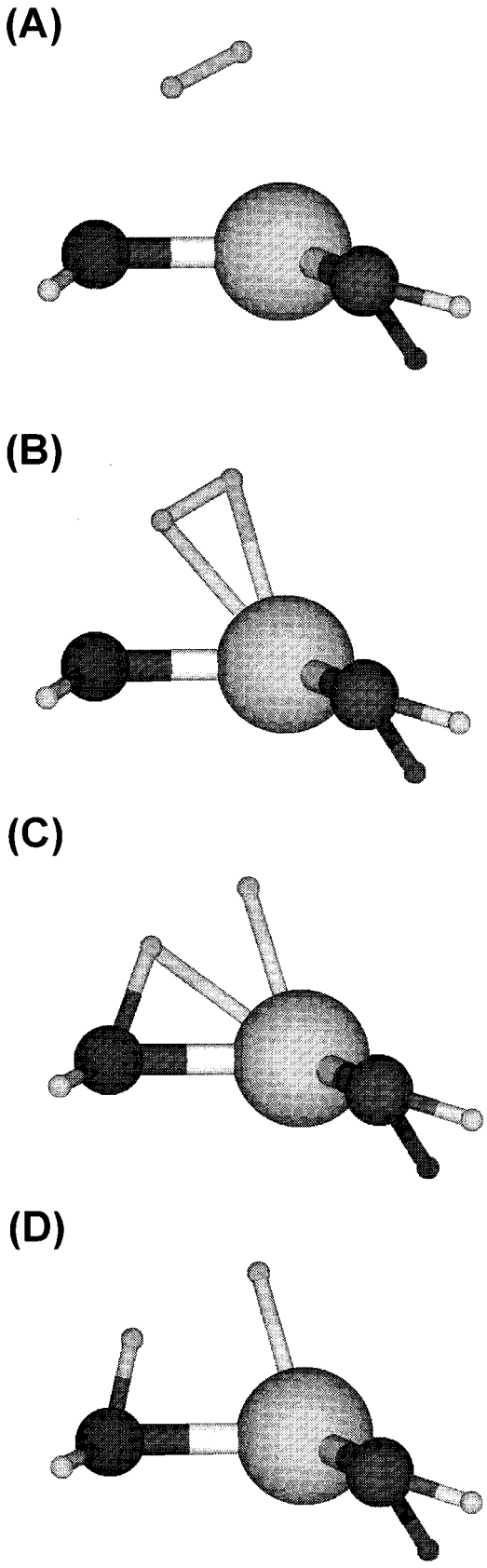

Figure 5. Snapshots of some structures along the reaction coordinate of hydrogen chemisorption on the tricoordinated aluminum cluster, taken between the physisorbed (Figure 2) and chemisorbed (Figure 3) states, calculated in mode B, at the B3LYP/6-31++G** level. **(C)** Transition structure (**11**).

TABLE 3: Changes in Bond Lengths Between Atoms Directly Involved in Chemisorption, Calculated at the B3LYP/6-31++G Level, in angstroms**

structure	*d*(Al−O)	*d*(H′−H)[a]	*d*(Al−H′)	*d*(Al−H)	*d*(O−H)
tricoordinated complex. Mode A, no symmetry constraint					
physisorbed complex (**2**)	1.71	0.75	2.28	2.30	2.94
transition structure (**11**)	1.88	1.12	1.75	1.83	1.18
chemisorbed complex (**3**)	2.05	1.87	1.62	2.30	0.98
tricoordinated complex. Mode B, no symmetry constraint					
physisorbed complex (**2**)	1.71	0.75	3.01	3.08	3.66
transition structure (**11**)	1.86	1.07	1.76	1.81	1.23
chemisorbed complex (**3**)	2.01	3.39	1.58	2.33	0.98
tetracoordinated complex					
physisorbed complex (**9**)	1.74	0.75	3.55	4.08	3.18
transition structure (**12**)	1.90	1.02	1.83	1.84	1.25
chemisorbed complex (**7a**)	2.13	2.71	1.60	2.66	0.97
pentacoordinated complex					
physisorbed complex (**10**)	1.76	0.74	5.42	6.09	4.49
transition structure (**13**)	1.97	1.07	1.82	1.86	1.21
chemisorbed complex (**8a**)	2.19	2.83	1.61	2.7	0.97

[a] H° farthest from Al; H′: closest to Al.

very close to the product **3**, giving an energy barrier, supposedly for desorption, of about 1 kcal/mol. For all the basis sets with diffuse functions, however, the transition structure had both hydrogen atoms within bonding distance of aluminum (1.75 and 1.83 Å), the shortest O···H distance at 1.2 Å, the H−H distance lengthened to more than 1.0 Å, and the Al−O bond lengthened to 1.9 Å. The latter transition structure is situated along the relevant reaction coordinate, as shown by the assignment of the specific vibration[21] of the imaginary frequency to the bending of one of the Al−H bonds toward the oxygen; that is, the migration of H from Al to O. It was, therefore, identified as **11** (Figure 5). The changes in the length of bonds directly involved in chemisorption from the physisorbed to the chemisorbed state are shown in Table 3. The alternative, **14**, was likewise identified[21] as the transition structure for the rotation of the Al−O bond and the corresponding energies are entered in parentheses in Table 1. These assignments were confirmed by IRC tracking at the MP2/6-31++G** level for **11** and at the MP2/6-31G** level for **14**. The transition structures obtained for the reaction of the cluster described in mode A with an imposed plane of symmetry were of the structure **11** for all basis sets. The transition structure for the reaction of the cluster in mode B was correctly identified with the basis set with or without diffuse functions (**11**B), and the IRC tracking conducted at the MP2/6-31G** level confirmed that they were positioned along the chemisorption reaction pathway.

For the reaction of the tetracoordinated aluminum cluster, the transition structure, **12** (Figure 6), was similar to **11**. Its identity was verified by IRC tracking at the B3LYP/6-31G** level. The pertinent interatomic distances shown in Table 3 indicate a reaction less advanced at the transition state than for the tricoordinated aluminum cluster. In the same way, the transition structure **13** was determined at the B3LYP/6-31G** and B3LYP/6-31++G** levels and tested by IRC tracking at the B3LYP/6-31G** level. The relevant interatomic distances in **13** are also given in Table 3.

The hydrogen dissociation on the $Al(OH)_3$ cluster model (**1**) was previously described as a strictly four-center process, with one hydrogen interacting with the aluminum and the other with the oxygen already in the physisorbed complex and the H−H bond being broken synchronously with the formation of the two new bonds.[7] Our calculations indicate, however, a different reaction mechanism. As shown in Figure 2 and Table 3, the hydrogen molecule (both atoms) interacts with the aluminum already in the physisorbed complex. The data in Table 3 show

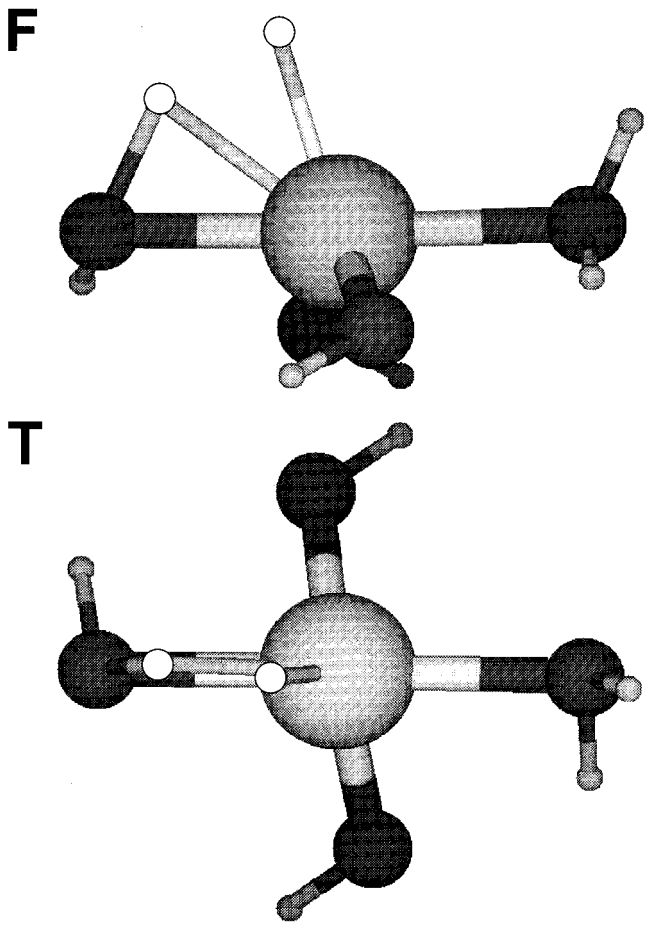

Figure 6. The geometry of the transition structure for the chemisorption of hydrogen on the tetracoordinated aluminum cluster at the B3LYP/6-31++G** level (**12**). F, T as in Figure 1.

that at the transition state the two Al−H distances in **11** are similar in length and only 8−16% longer than the Al−H bond in the chemisorbed complex. The shortest O−H distance is 20−29% longer in the transition structure than in the chemisorbed complex. At the same time, the H−H distance is 36−49% longer in the transition structure than in the physisorbed complex, indicating that the bond has cleaved.

Examination of the changes in geometry along the reaction coordinates indicates that the hydrogen molecule interacts at

first with the aluminum atom for all the clusters (**1**, **5**, and **6**). For example, IRC tracking for the reaction of **1** in mode A at the MP2/6-31++G** was used to elucidate the pathway for **2** → **11** → **3** (Figure 5, A, B, C, D). It shows the hydrogen molecule moving toward the aluminum atom. The hydrogen which is to be bonded to oxygen reaches the same distance as in the transition structure (Al−H 1.83 Å, 13% longer than in **3**) when the H−H bond (0.8 Å) is stretched only by 7% and the Al−O bond (1.86 Å) is stretched by 9%. Thus, a three-center bond is formed in the first stage of chemisorption (the other distance, Al−H′, is 1.86 Å). At that point, the shortest O−H distance is 1.53 Å, 56% longer than in **3**. Both aluminum−hydrogen bonds continue to contract until they reach Al−H = Al−H′ = 1.80 Å, which is 11% longer than Al−H′ in **3**. At that point, the H−H bond (0.87 Å) is already stretched by 16%, the Al−O (1.87 Å) is still only 9% longer than in **3**, whereas the O−H distance is 1.40 Å (43% elongation). Then the migration of H from Al to O occurs, with the Al−H distance increasing, the O−H distance decreasing, and the Al−O distance staying the same until they reach the values shown in Table 3 for the transition structure **11**, then continuing smoothly to **3**. The representation of hydrogen dissociation as a heterolysis by interaction with both aluminum (positive) and oxygen (negative)[7] is not substantiated by the higher-level calculations. Instead, the reaction appears to be an example of metal ion catalysis.

Conclusions

Our results indicate that all aluminum sites with coordination lower than six can participate in the dissociative chemisorption of hydrogen. The reactivity, judged by the energy of the transition structure for chemisorption relative to reactants, decreases with the increase in the number of ligands previously attached to the aluminum atom: $Al(-O-)_3 > Al(-O-)_4 > Al(-O-)_5$. That tetracoordinated aluminum sites have to be considered reactive sites is important, particularly considering that a significant fraction of the aluminum atoms in transitional aluminas are tetracoordinated.[21,28]

For the tricoordinated sites, the stability of the chemisorbed complex is influenced significantly by the geometry, especially the closeness to planarity, and by the flexibility of the aluminum center, but the energy barrier for chemisorption does not change much with these structural factors.

The reaction is not an acid−base catalysis involving the heterolysis of the H−H bond, but it is a case of metal ion catalysis, with hydrogen chemisorption occurring on aluminum, followed by the migration of one of the hydrogens from aluminum to oxygen.

The DFT-B3LYP calculations give results similar to those obtained by MP2 calculations and are, therefore, adequate for this type of problem. It should be noted, however, that in all cases but one the relative energies for the chemisorbed complexes and the corresponding transition structures were lower when calculated by the B3LYP than by the MP2 method. Basis sets of appropriate size should be used with either method, and introduction of diffuse functions in the basis sets seems necessary. Even though erroneous results were obtained only in some limited cases with basis sets without diffuse functions, one cannot know in advance when the results would be reliable and when not.

Acknowledgment. Our research of strong acid catalysis is supported by Grant CTS-9528412 from NSF. A grant of supercomputer time was obtained from the National Center for Supercomputing Applications (NCSA) in Urbana, IL. We are indebted to Prof. Kenneth D. Jordan and Dr. Douglas J. Fox for many helpful discussions, and to Dr. Balaji Veeraraghavan and Dr. Sudhakhar Pamidighantam for helping us with the use of the Gaussian 94 program at NCSA.

References and Notes

(1) (a) Taylor, H. S.; Diamond, H. *J. Am. Chem. Soc.* **1935**, *57*, 1256. (b) Lee, J. K.; Weller, S. W. *Anal. Chem.* **1958**, *30*, 1057. (c) Hall, W. K.; Leftin, H. P.; Cheselske, F. J.; O′Reilly, D. E. *J. Catal.* **1963**, *2*, 506. (d) Hall, W. K.; Lutinski, F. E. *J. Catal.* **1963**, *2*, 518. (e) Carter, J.; Lucchesi, P.; Corneil, P.; Yates, D. J. C.; Sinfelt, J. H. *J. Phys. Chem.* **1965**, *69*, 3070.

(2) (a) Vannice, M. A.; Neikan, W. C. *J. Catal.* **1971**, *20*, 260. (b) Levy, R. V.; Boudart, M. *J. Catal.* **1974**, *32*, 304. (c) Fleisch, T.; Aberman, R. *J. Catal.* **1977**, *50*, 268. (d) Musso, J. C.; Parera, J. M. *Appl. Catal.* **1987**, *30*, 81.

(3) (a) Khoobiar, S. *J. Phys. Chem.* **1964**, *68*, 411. (b) Robell, A. J.; Ballou, E. V.; Boudart, M. *J. Phys. Chem.* **1964**, *68*, 2748. (c) Review: Conner, W. C., Jr.; Pajonk, G. M.; Teichner, S. J. *Adv. Catal.* **1986**, *34*, 1. (d) A case was reported where the phenomenon consisted of reduction of the support, rather than formation of hydrogen atoms adsorbed on it: Sachtler, W. M. H. *Topics in Catalysis*; Baltzer Scientific: Amsterdam, 1999, in press.

(4) (a) V. B. Kazansky, *Stud. Surf. Sci. Catal.* **1991**, *65*, 117. (b) Ioka, F.; Sakka, T.; Ogata, Y.; Iwasaki, M. *Can. J. Chem.* **1993**, *71*, 663. (c) See also: Perry, J. B. *J. Phys. Chem.*, **1965**, *69*, 220.

(5) Weller, S. W.; Montagna, A. A. *J. Catal.* **1971**, *201*, 303.

(6) Zelenovskii, V. M.; Zhidomirov, G. M.; Kazanskii, V. B. *Zh. Fiz. Khim.* **1984**, *58*, 1788.

(7) Senchenya, I. N.; Kazanskii, V. B. *Kinet. Katal.* **1988**, *29*, 1331.

(8) (a) Pople, J. *Acc. Chem. Res.* **1970**, 3, 217. (b) Pople, J. A. *Int. J. Mass Spectrom. Ion Phys.* **1976**, *19*, 89. (c) Hehre, W. J.; Radom, L.; Schleyer, P. v. R.; Pople, J. A. *Ab Initio Molecular Orbital Theory*; Wiley-Interscience: New York, 1986.

(9) Fărcaşiu, D.; Norton, S. H. *J. Org. Chem.* **1997**, *62*, 5374.

(10) See the discussion in: Schwarz, K.; Nusterer, E.; Blöchl, P. E. *Catal. Today* **1999**, *50*, 501.

(11) Sauer, J.; Ugliengo, P.; Garrone, G.; Saunders: V. R. *Chem. Rev.* **1994**, *94*, 2095.

(12) (a) Fărcaşiu, D.; Hâncu, D. *J. Phys. Chem.* **1997**, *101*, 8695, esp. ref 40. (b) Other examples of nonperformance of DFT calculations have been reported: Boronat, M.; Viruela, P.; Corma, A. *J. Phys. Chem.* **1997**, *101*, 10069.

(13) Frisch, M. J.; Trucks, G. W.; Schlegel, H. B.; Gill, P. M. W.; Johnson, B. G.; Robb, M. A.; Cheeseman, J. R.; Keith, T.; Petersson, G. A.; Montgomery, J. A.; Raghavachari, K.; Al-Laham, M. A.; Zakrzewski, V. G.; Ortiz, J. V.; Foresman, J. B.; Cioslowski, J.; Stefanov, B. B.; Nanayakkara, A.; Challacombe, M.; Peng, C. Y.; Ayala, P. Y.; Chen, W.; Wong, M. W.; Andres, J. L.; Replogle, E. S.; Gomperts, R.; Martin, R. L.; Fox, D. J.; Binkley, J. S.; DeFrees, D. J.; Baker, J.; Stewart, J. P.; Head-Gordon, M.; Gonzalez, C.; Pople, J. A. *Gaussian 94, Revision D.3*; Gaussian, Inc.: Pittsburgh, PA, 1995.

(14) Fărcaşiu, D.; Lukinskas, P. *J. Phys. Chem. A* **1998**, *102*, 10436.

(15) (a) Hohenberg, P.; Kohn, W. *Phys. Rev.* **1964**, *136*, B864. (b) Kohn, W.; Sham, L. *Phys. Rev.* **1965**, *140*, A1133. (c) Parr, R. G.; Yang, W. *Density Functional Theory of Atoms and Molecules*; Oxford University Press: New York, 1989. (d) Becke, A. D. *J. Chem. Phys.* **1993**, *98*, 5648.

(16) Chalasiński, G.; Gutowski, M. *Chem. Rev.* **1988**, *88*, 943.

(17) (a) Alagona, G.; Ghio, C.; Tomasi, J. *J. Phys. Chem.* **1989**, *93*, 5401. (b) Alagona, G.; Ghio, C. *J. Comput. Chem.* **1990**, *11*, 930.

(18) Peng, C.; Schlegel, H. B. *Israel J. Chem.* **1993**, *33*, 449.

(19) Gonzales, C.; Schlegel, H. B. *J. Phys. Chem.* **1989**, *90*, 2154.

(20) *Xmol, version 1.3.1*; Minnesota supercomputing Center, Inc.: Minneapolis, MN, 1993.

(21) Schaftenaar, G. MOLDEN. A Portable Electron Density Program, QCPE 619; *QCPE Bull.* **1992**, *12*, 3.

(22) Knözinger, H.; Ratnasamy, P. *Catal. Rev. Sci. Eng.* **1978**, *17*, 31.

(23) Bandiera, J.; Naccache, C. *Bull. Soc. Chim. France* **1969**, 2637.

(24) Coster, D.; Blumenfeld, A. L.; Fripiat, J. J. *J. Phys. Chem.* **1994**, *98*, 6201.

(25) Huggins, B. A.; Ellis, P. D. *J. Am. Chem. Soc.* **1992**, *114*, 2098.

(26) Ripmeester, J. A. *J. Am. Chem. Soc.* **1983**, *105*, 2925.

(27) 1 cal = 4.184 J.

(28) Lee, M.-H.; Cheng, C.-F.; Heine, V.; Klinowski, J. *Chem. Phys. Lett.* **1997**, *265*, 673.